Electronic supplementary information for
Floppy molecules as candidates for achieving optoelectronic molecular devices without skeletal rearrangement or bond breaking

Ioan Bâldea * [a‡]

Keywords: nanotechnology; molecular optoelectronics; photoswitch; nanojunctions; molecular photoresistance; floppy molecules

S1 Impact of the torsional angle on the low-bias conductance

Because of the key role played by eqn (1) of the main text in the present study, a few words on its justification may be useful.

(i) First and foremost, eqn (1) has been straightforwardly validated in experiments on nanojunctions based on molecules consisting of two rings [1–3]. This represents the most direct justification of the fact that the dependence $t \propto \cos\varphi$ predicted by the molecular orbital (MO) theory [4] for the electron transfer integral t between the two rings plays the leading role in determining the scaling $G \propto \cos^{\varphi}$, which prevails over other possible changes brought about φ-variations, like, *e.g.*, changes $\varepsilon_{MO} = \varepsilon_{MO}(\varphi)$ in MO energies.

(ii) The dependence expressed by eqn (1) is supported by DFT calculations (*cf.* Fig. 2a of ref. 5), which account for possible dependencies $\varepsilon_{MO} = \varepsilon_{MO}(\varphi)$.

(iii) The derivation of eqn (1) can be done analytically within a theoretical model presented below. The demonstration that follows emphasizes the leading role played by the transfer integral t in determining the behavior of G and the fact that modifications in MO energies are quantitatively negligible.

The model assumes that each of the two rings ($j = 1,2$) is described by a energy level (MO) associated with the dominant transport channel. The MO energies $\varepsilon_{1,2} = \varepsilon_0$ of the isolated rings — measured relative to the Fermi energy ($E_F = 0$) of the unbiased electrodes — are assumed equal for simplicity. The electron transfer between the two rings is quantified by the transfer integral t, a quantity already introduced in the main text.

The Landauer trace formula [4] can be straightforwardly applied to this model to obtain the following expression of the low bias conductance G

$$g_2 \equiv \frac{G}{G_0} = \frac{t^2\Gamma^2}{\left|\left(\varepsilon_0 - \frac{i}{2}\Gamma\right)^2 - t^2\right|^2} \tag{S1}$$

where g_2 is the conductance of the two-ring system in units of quantum conductance $G_0 = 2e^2/h = 1/(12.9\,\mathrm{k\Omega})$ and Γ is the molecule-electrode coupling.

In situations of practical interest (corresponding to off-resonant tunneling), the MO energy offsets are substantially larger than the molecule-electrode couplings and the inter-ring transfer integral

$$\Gamma^2 \ll \varepsilon_0^2,\ t^2 \ll \varepsilon_0^2 \tag{S2}$$

In such cases, the right hand side (RHS) of eqn (S1) gets a simpler form

$$g_2 = \frac{G}{G_0} \approx t^2\frac{\Gamma^2}{\varepsilon_0^2} \tag{S3}$$

Eqn (1) of the main text follows from the above result because

$$t \propto \cos\varphi \tag{S4}$$

To justify the assumptions of eqn (S2), let us refer to the case of the recently studied molecular junctions based oligophenylene dithiols [6]. Numerical data used below are taken from Table 1 of ref. 6.

For benzene dithiol junctions (denoted by OPD1 in ref. 6), a conductance per molecule

$$g_{OPD1} = (12.9/6.06)/80 = 0.0266 \tag{S5}$$

can be deduced from the resistance $R = 6.06\,\mathrm{k\Omega}$ of the CP-AFM (conducting probe atomic force microscope) junctions consisting of bundles of $N = 80$ OPD1 molecules. Modelling OPD1 in a manner similar to that delineated above, namely as a consisting of a single ring/level of energy ε_0, its normalized conductance can be expressed in the well known form [4]

$$g_1 \approx \frac{\Gamma^2}{\varepsilon_0^2} \tag{S6}$$

[a] *Theoretische Chemie, Universität Heidelberg, Im Neuenheimer Feld 229, D-69120 Heidelberg, Germany.*
‡ E-mail: ioan.baldea@pci.uni-heidelberg.de. Also at National Institute for Lasers, Plasmas, and Radiation Physics, Institute of Space Sciences, RO 077125, Bucharest-Măgurele, Romania

Let us note at this point that eqn (S6) and (S3) can be combined as

$$\frac{g_2}{g_1} \approx \frac{t^2}{\varepsilon_0^2} \tag{S7}$$

With the value $g_1 \equiv g_{OPD1}$ of eqn (S5), eqn (S6) yields $\Gamma^2/\varepsilon_0^0 = 0.0266$, a value that justifies the first part of eqn (S2).

For biphenyl dithiol junctions (denoted by OPD2 in ref. 6), a conductance per molecule

$$g_{OPD2} = (12.9/26.86)/82 = 0.00586 \tag{S8}$$

can be deduced from the resistance $R = 26.83\,\mathrm{k}\Omega$ of the CP-AFM (conducting probe atomic force microscope) junctions consisting of bundles of $N \simeq 82$ OPD2 molecules. Noting that OPD2 is a molecule consisting of two rings of the kind considered above, we can use eqn (S7) with values $g_2 \equiv g_{OPD2}$ and $g_1 \equiv g_{OPD1}$ taken from eqn (S8) and (S5) to derive the following result

$$\frac{g_2}{g_1} = \frac{t^2}{\varepsilon_0^2} = 0.22 \tag{S9}$$

which justifies the second part of eqn (S2).

Before ending this issue, let us still note that a nonvanishing inter-ring electron transfer ($t \neq 0$) modifies the level energies of the isolated rings ($\varepsilon_{1,2} \rightarrow \tilde{\varepsilon}_{1,2}$). The general expression reads

$$\tilde{\varepsilon}_{1,2} = \frac{\varepsilon_1 + \varepsilon_2}{2} \pm \sqrt{\left(\frac{\varepsilon_1 - \varepsilon_2}{2}\right)^2 + t^2} \tag{S10}$$

The dependence on t of the RHS of eqn (S10) expresses the physical fact that the energy levels of a two-ring molecule depend on the torsional angle (*cf.*eqn S4). In fact, the differences between the denominators entering eqn (S1) and (S3) mathematically reflect just the differences between $\tilde{\varepsilon}_{1,2}$ and $\varepsilon_{1,2}$. Therefore, with the specific example examined above, we have demonstrated that, although the MO energies $\tilde{\varepsilon}_{1,2}$ exhibit a certain φ-dependence — arising *via* t entering the RHS of eqn (S10) — the corresponding impact on G is not considerable; the leading contribution to the scaling of eqn (1) arises *via* the quantity t^2 entering the numerator of eqn (S1) or (S3).

S2 Cartesian coordinates

Cartesian coordinates of the three molecular species considered in this paper are collected in Tables S1, S2, S3, S4, S5, and S6.

S3 Bond metric data

Detailed bond metric data for the 44BPY, 2BMT, and BMT-PY methods, allowing to better assess similarities and differences between the geometries optimized by the various methods utilized in this paper, are collected in Tables S7, S8, and S9, respectively.

S4 Vertical and adiabatic excitation energy

The lowest excitation energies for vertical and adiabatic processes computed *ab initio* are presented in Table S10.

S5 LUMO spatial distributions

The LUMO spatial distributions of the two other molecular species (44BPY and 2BMT) not shown in the main text are depicted in Figure S1 and S2. Like in Figure 2 of the main text, we present there along the LUMO distribution obtained within SCF calculations (left panels) also the LUMO distribution computed from the natural orbital expansion of the corresponding reduced density matrices of the anionic species at the EOM-CCSD (equation-of-motion coupled-cluster singles and doubles[7,8]) calculations by using CFOUR[9]; see, *e.g.*, ref. 10 and citations therein. The reason for also conducting calculation at the second, more elaborate level of theory is the following. First, let us remind that unoccupied (or virtual) Hartree-Fock (HF) MOs (in particular, the LUMO) might have physical meaning, *e.g.*, in describing anionic bound or resonance states, provided that the basis set size is not too large. (This is why, in conjunction with the left panels of Figure S1, Figure S2, and Figure 2 of the main text, we utilized the smaller 6-31+g(d,p) basis sets instead of the larger aug-cc-pVDZ basis sets employed in the other calculations.) However, for larger basis sets needed in accurate quantum chemical calculations, the LUMO (as well as other unoccupied HF orbitals) have mathematical rather than physical significance[10,11]. The fact that the spatial distributions of the left and middle panels of Figure S2 are hard to distinguish suggests that for 2BMT calculations at not so high levels of theory may suffice.

Notes and references

1 L. Venkataraman, J. E. Klare, C. Nuckolls, M. S. Hybertsen and M. L. Steigerwald, *Nature*, 2006, **442**, 904 – 907.

2 D. Vonlanthen, A. Mishchenko, M. Elbing, M. Neuburger, T. Wandlowski and M. Mayor, *Angew. Chem. Int. Ed.*, 2009, **48**, 8886–8890.

3 A. Mishchenko, D. Vonlanthen, V. Meded, M. Bürkle, C. Li, I. V. Pobelov, A. Bagrets, J. K. Viljas, F. Pauly, F. Evers, M. Mayor and T. Wandlowski, *Nano Lett.*, 2010, **10**, 156–163.

4 J. C. Cuevas and E. Scheer, *Molecular Electronics: An Introduction to Theory and Experiment*, World Scientific Publishers, 2010.

5 H. Kondo, J. Nara, H. Kino and T. Ohno, *J. Chem. Phys.*, 2008, **128**, 064701.

6 Z. Xie, I. Bâldea, A. T. Demissie, C. E. Smith, Y. Wu, G. Haugstad and C. D. Frisbie, *J. Am. Chem. Soc.*, 2017, **139**, 5696–5699.

7 J. F. Stanton and J. Gauss, *J. Chem. Phys.*, 1994, **101**, 8938–8944.

8 M. Nooijen and R. J. Bartlett, *J. Chem. Phys.*, 1995, **102**, 3629–3647.

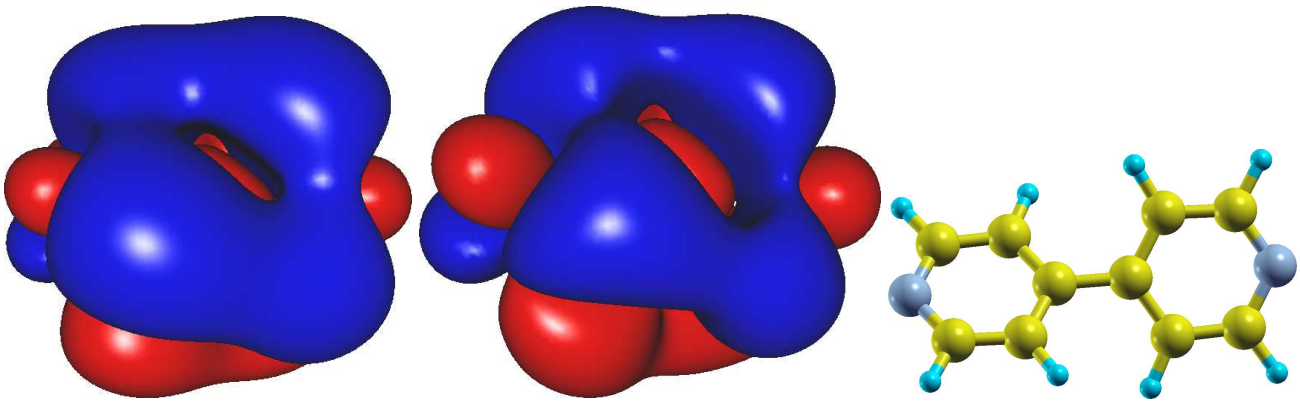

Fig. S1 Left panel: the spatial distribution of the LUMO of the 44BPY molecule obtained *via* SCF/6-31+g(d,p)[12] calculations. Middle panel: the spatial distribution of the singly occupied natural orbital exhausting 97.7% of the excess electron density in $44BPY^{\bullet-}$ radical anion ("LUMO") obtained *via* calculations based on the equation-of-motion couple-cluster singles and doubles and aug-cc-pVDZ basis sets for all atoms (EA-EOM-CCSD/aug-cc-pVDZ) with CFOUR[9]. Right panel (generated with XCrysDen[13]): molecular orientation. Apart for certain differences between the two panels, which reflect the different levels of theory utilized, both panels reveals that the LUMO is delocalized over the whole molecule. This fact enhances the π-interaction favoring thereby a planar conformation. Figures generated with GABEDIT[14].

9 CFOUR, Coupled-Cluster Techniques for Computational Chemistry, a Quantum-Chemical Program Package by J.F. Stanton, J. Gauss, M.E. Harding, P.G. Szalay with contributions from A.A. Auer, R.J. Bartlett, U. Benedikt, C. Berger, D.E. Bernholdt, Y.J. Bomble, L. Cheng, O. Christiansen, M. Heckert, O. Heun, C. Huber, T.-C. Jagau, D. Jonsson, J. Jusélius, K. Klein, W.J. Lauderdale, D.A. Matthews, T. Metzroth, L.A. Mück, D.P. O'Neill, D.R. Price, E. Prochnow, C. Puzzarini, K. Ruud, F. Schiffmann, W. Schwalbach, C. Simmons, S. Stopkowicz, A. Tajti, J. Vázquez, F. Wang, J.D. Watts and the integral packages MOLECULE (J. Almlöf and P.R. Taylor), PROPS (P.R. Taylor), ABACUS (T. Helgaker, H.J. Aa. Jensen, P. Jørgensen, and J. Olsen), and ECP routines by A. V. Mitin and C. van Wüllen. For the current version, see http://www.cfour.de.

10 I. Bâldea, *Faraday Discuss.*, 2014, **174**, 37–56.

11 I. Bâldea, *Nanoscale*, 2013, **5**, 9222–9230.

12 M. J. Frisch, G. W. Trucks, H. B. Schlegel, G. E. Scuseria, M. A. Robb, J. R. Cheeseman, G. Scalmani, V. Barone, B. Mennucci, G. A. Petersson, H. Nakatsuji, M. Caricato, X. Li, H. P. Hratchian, A. F. Izmaylov, J. Bloino, G. Zheng, J. L. Sonnenberg, M. Hada, M. Ehara, K. Toyota, R. Fukuda, J. Hasegawa, M. Ishida, T. Nakajima, Y. Honda, O. Kitao, H. Nakai, T. Vreven, J. A. Montgomery, Jr., J. E. Peralta, F. Ogliaro, M. Bearpark, J. J. Heyd, E. Brothers, K. N. Kudin, V. N. Staroverov, T. Keith, R. Kobayashi, J. Normand, K. Raghavachari, A. Rendell, J. C. Burant, S. S. Iyengar, J. Tomasi, M. Cossi, N. Rega, J. M. Millam, M. Klene, J. E. Knox, J. B. Cross, V. Bakken, C. Adamo, J. Jaramillo, R. Gomperts, R. E. Stratmann, O. Yazyev, A. J. Austin, R. Cammi, C. Pomelli, J. W. Ochterski, R. L. Martin, K. Morokuma, V. G. Zakrzewski, G. A. Voth, P. Salvador, J. J. Dannenberg, S. Dapprich, A. D. Daniels, O. Farkas, J. B. Foresman, J. V. Ortiz, J. Cioslowski, and D. J. Fox, Gaussian, Inc., Wallingford CT, 2010 Gaussian 09, Revision B.01.

13 A. Kokalj, *Comp. Mater. Sci.*, 2003, **28**, 155 – 168.

14 A.-R. Allouche, *J. Comput. Chem.*, 2011, **32**, 174–182.

Atom	X	Y	Z
C	1.0813020	0.3973692	2.8801355
C	1.1328313	0.4159663	1.4745737
C	-1.1328313	-0.4159663	1.4745737
C	-1.0813020	-0.3973692	2.8801355
N	0.0000000	0.0000000	3.5963175
H	1.9477057	0.7225625	3.4664847
H	2.0316799	0.7721099	0.9609315
H	-2.0316799	-0.7721099	0.9609315
H	-1.9477057	-0.7225625	3.4664847
C	0.0000000	0.0000000	-0.7408548
C	1.1328313	-0.4159663	-1.4745737
C	-1.1328313	0.4159663	-1.4745737
C	1.0813020	-0.3973692	-2.8801355
H	2.0316799	-0.7721099	-0.9609315
C	-1.0813020	0.3973692	-2.8801355
H	-2.0316799	0.7721099	-0.9609315
N	0.0000000	0.0000000	-3.5963175
H	1.9477057	-0.7225625	-3.4664847
H	-1.9477057	0.7225625	-3.4664847
C	0.0000000	0.0000000	0.7408548

Table S1 Cartesian coordinates in angstrom of the 44BPY molecule in the neutral ground state as obtained from CC2/aug-cc-pVDZ calculations.

Atom	X	Y	Z
C	0.0244540	1.2216559	2.8851532
C	0.0244846	1.2364854	1.4954729
C	-0.0249373	-1.2364829	1.4954685
C	-0.0253466	-1.2216480	2.8851489
N	-0.0005433	0.0000044	3.4752620
H	0.0496971	2.1140458	3.5149348
H	0.0523428	2.2198089	1.0197649
H	-0.0526394	-2.2198081	1.0197550
H	-0.0507854	-2.1140367	3.5149246
C	0.0001116	-0.0000006	-0.7166719
C	-0.0247930	1.2068588	-1.4866125
C	0.0252514	-1.2068617	-1.4866018
C	-0.0222766	1.1473772	-2.8863020
H	-0.0493699	2.1911276	-1.0098144
C	0.0231605	-1.1473839	-2.8862923
H	0.0496827	-2.1911293	-1.0097934
N	0.0005533	-0.0000043	-3.6189951
H	-0.0420425	2.0784050	-3.4649964
H	0.0431033	-2.0784131	-3.4649781
C	-0.0001086	0.0000006	0.7251731

Table S2 Cartesian coordinates in angstrom of the 44BPY neutral molecule in its lowest electronically excited state as obtained from CC2/aug-cc-pVDZ calculations.

Atom	X	Y	Z
C	1.7376227	-1.1860683	0.4215087
C	3.1451560	-1.1866995	0.4195657
C	3.8543817	-0.0483677	-0.0141500
C	3.1455925	1.0899128	-0.4486926
C	1.7380508	1.0891581	-0.4520869
C	1.0168823	-0.0484171	-0.0155637
H	1.1901757	-2.0615647	0.7870788
H	3.6886825	-2.0709731	0.7673269
H	3.6894686	1.9741595	-0.7960028
H	1.1909529	1.9644951	-0.8185975
C	-0.4652834	-0.0485521	-0.0161268
C	-1.1921851	1.0899495	0.4048887
C	-1.1924274	-1.1875393	-0.4375073
C	-2.5983320	1.0952109	0.4059257
H	-0.6523038	1.9741674	0.7606743
C	-2.5977042	-1.1916067	-0.4385488
H	-0.6522920	-2.0714110	-0.7934608
C	-3.3130127	-0.0474476	-0.0164490
H	-3.1364338	1.9853593	0.7486023
H	-3.1403567	-2.0795307	-0.7804071
S	-5.0970633	-0.1287733	-0.0404255
H	-5.3082571	1.1429459	0.3661567
H	4.9486856	-0.0484071	-0.0137089

Table S3 Cartesian coordinates in angstrom of the 2BMT molecule in the neutral ground state as obtained from CC2/aug-cc-pVDZ calculations.

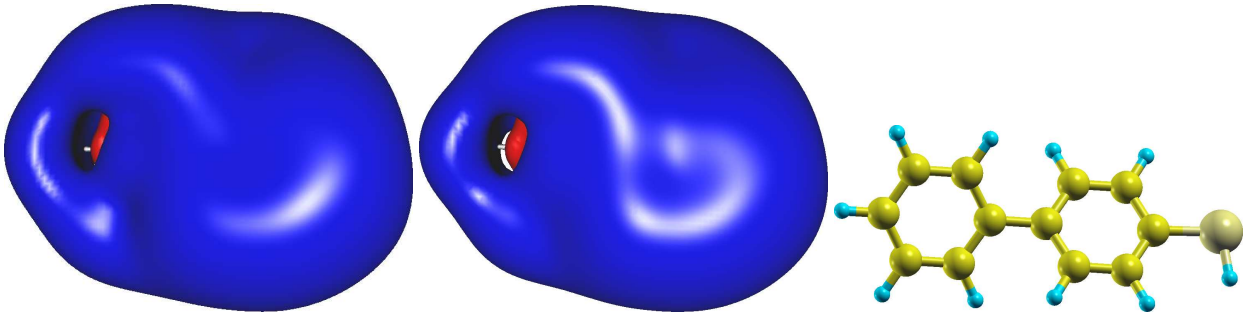

Fig. S2 Left panel: the spatial distribution of the LUMO of the 2BMT molecule obtained *via* SCF/6-31+g(d,p) [12] calculations. Middle panel: the spatial distribution of the singly occupied natural orbital exhausting 95.6% of the excess electron density in $2BMT^{\bullet-}$ radical anion ("LUMO") obtained *via* calculations based on the equation-of-motion couple-cluster singles and doubles and aug-cc-pVDZ basis sets for all atoms (EA-EOM-CCSD/aug-cc-pVDZ) with CFOUR [9]. Right panel (generated with XCrysDen [13]): molecular orientation. Apart for certain differences between the first two panels, which reflect the different levels of theory utilized, both panels reveals that the LUMO is delocalized over the whole molecule. This fact enhances the π-interaction favoring thereby a planar conformation. Figures generated with GABEDIT [14].

Atom	X	Y	Z
C	1.7396406	-1.2745751	-0.0244965
C	3.1488850	-1.2688343	-0.0370374
C	3.8556567	-0.0452015	-0.0347113
C	3.1453681	1.1772350	-0.0197304
C	1.7366388	1.1774673	-0.0071461
C	0.9992690	-0.0492399	-0.0092249
H	1.2185165	-2.2331001	-0.0265979
H	3.6951376	-2.2168402	-0.0486123
H	3.6884181	2.1270791	-0.0178562
H	1.2131491	2.1348035	0.0042727
C	-0.4555368	-0.0534168	0.0037311
C	-1.1887939	1.1891988	0.0191439
C	-1.1835087	-1.3004455	0.0012866
C	-2.6180648	1.1964388	0.0318660
H	-0.6641317	2.1450335	0.0214820
C	-2.6142187	-1.3025697	0.0140668
H	-0.6590006	-2.2557694	-0.0102977
C	-3.3144089	-0.0555241	0.0291667
H	-3.1735529	2.1388045	0.0436206
H	-3.1732091	-2.2433863	0.0122647
S	-5.0627397	-0.1398353	0.0443224
H	-5.2839096	1.1964331	0.0549574
H	4.9503957	-0.0437555	-0.0444701

Table S4 Cartesian coordinates in angstrom of the neutral 2BMT molecule in its lowest electronically excited state obtained from CC2/aug-cc-pVDZ calculations.

Atom	X	Y	Z
C	1.9800468	-1.1554400	-0.3895783
C	0.5753619	-1.1523182	-0.3872908
C	-0.1490869	0.0003182	-0.0008371
C	0.5752665	1.1522924	0.3853601
C	1.9808514	1.1564388	0.3878031
C	2.6952190	0.0011196	-0.0007349
H	2.5228264	-2.0531618	-0.7041083
H	0.0353550	-2.0468903	-0.7151954
H	0.0356151	2.0472305	0.7131797
H	2.5190367	2.0563370	0.7032601
S	4.4776098	-0.0806379	-0.0257724
H	4.6894814	1.1916547	0.3787421
C	-1.6293113	0.0005762	-0.0001676
C	-2.3681114	1.1288921	-0.4235503
C	-2.3678630	-1.1276696	0.4238470
C	-3.7733792	1.0793995	-0.4007406
H	-1.8570290	2.0248849	-0.7907444
C	-3.7731503	-1.0777949	0.4026168
H	-1.8565709	-2.0238872	0.7901552
N	-4.4917796	0.0008755	0.0013144
H	-4.3586633	1.9453722	-0.7296501
H	-4.3582561	-1.9436158	0.7322146

Table S5 Cartesian coordinates of the neutral BMT-PY molecule in the ground state as obtained from CC2/aug-cc-pVDZ calculations.

Atom	X	Y	Z
C	2.4067145	-1.3029642	0.0242750
C	0.9703423	-1.3128830	-0.0044708
C	0.2464264	-0.0603042	0.0025002
C	0.9813075	1.1794013	0.0241679
C	2.4087677	1.1995265	0.0280360
C	3.1080271	-0.0568494	0.0432675
H	2.9694087	-2.2419116	0.0181839
H	0.4477947	-2.2687628	-0.0371940
H	0.4484671	2.1314389	0.0513554
H	2.9587011	2.1439633	0.0641241
S	4.8509468	-0.1374043	0.1297291
H	5.0741175	1.1865280	-0.0631472
C	-1.2110039	-0.0475618	-0.0116266
C	-1.9670632	1.1607861	-0.0197739
C	-1.9688302	-1.2563376	-0.0211465
C	-3.3725620	1.1078057	-0.0347290
H	-1.4817746	2.1390923	-0.0154087
C	-3.3754915	-1.1963848	-0.0362641
H	-1.4839001	-2.2342461	-0.0152811
N	-4.0960508	-0.0456175	-0.0427571
H	-3.9543786	2.0357244	-0.0403678
H	-3.9599665	-2.1230392	-0.0434724

Table S6 Cartesian coordinates of the neutral BMT-PY molecule in its lowest electronically excited state as obtained from CC2/aug-cc-pVDZ calculations.

Species, Method	N_1C_3	C_3C_5	C_5C_7	C_7C_8	N_2C_4	C_4C_6	C_6C_8	N_1N_2	φ_1
n, CC2	1.3565	1.4066	1.4123	1.4817	1.3565	1.4066	1.4123	7.1926	40.3
n, DFT/B3LYP	1.3400	1.3965	1.4037	1.4844	1.3400	1.3965	1.4037	7.1499	37.3
a, DFT/B3LYP	1.3581	1.3848	1.4370	1.4348	1.3581	1.3848	1.4370	7.2667	0.0
e, TD-DFT/B3LYP	1.3330	1.3829	1.4424	1.4403	1.3330	1.3829	1.4424	7.0551	0.0
e, CCS	1.3369	1.3739	1.4458	1.4038	1.3369	1.3739	1.4457	7.0960	0.0
e, ADC(2)	1.3706	1.3909	1.4624	1.4062	1.3706	1.3909	1.4622	7.2053	0.0
e, CC2	1.3615	1.4010	1.4318	1.4419	1.3569	1.3897	1.4570	7.0946	0.0

Species, Method	N_1C_{11}	$C_{11}C_9$	C_9C_7	C_7C_8	N_2C_{12}	$C_{12}C_{10}$	$C_{10}C_8$	N_1N_2	φ_2
n, CC2	1.3565	1.4066	1.4123	1.4817	1.3565	1.4066	1.4123	7.1926	40.3
n, DFT/B3LYP	1.3400	1.3965	1.4037	1.4844	1.3400	1.3965	1.4037	7.1499	37.3
a, DFT/B3LYP	1.3581	1.3848	1.4370	1.4348	1.3581	1.3848	1.4370	7.2667	0.0
e, TD-DFT/B3LYP	1.3330	1.3829	1.4424	1.4403	1.3330	1.3829	1.4424	7.0551	0.0
e, CCS	1.3369	1.3739	1.4458	1.4038	1.3369	1.3739	1.4457	7.0960	0.0
e, ADC(2)	1.3706	1.3909	1.4624	1.4062	1.3706	1.3909	1.4622	7.2053	0.0
e, CC2	1.3615	1.4010	1.4318	1.4419	1.3569	1.3898	1.4570	7.0946	0.0

Table S7 Results for 44BPY. The first letters n, a, and e in the left column indicate that the results of the corresponding rows refer to the optimized geometries of the the neutral ground state, anionic ground state, and the lowest excited state of the neutral molecule, respectively. $\varphi_1 \equiv [C_5C_7C_8C_6]$ and $\varphi_2 \equiv [C_9C_7C_8C_{10}]$ represent the torsional angles formed by the two planes specified by the C atoms indicated in the square brackets. Atom labeling is indicated in Figure 1A. Throughout, lengths are given in angstrom and angles in degrees.

Species, Method	C_1C_3	C_3C_5	C_5C_7	C_7C_8	C_2C_4	C_4C_6	C_6C_8	C_2S	C_1S	φ_1
n, CC2	1.4096	1.4075	1.4159	1.4822	1.4138	1.4053	1.4155	1.7861	8.9519	41.3
n, DFT/B3LYP	1.3985	1.3966	1.4075	1.4852	1.4028	1.3943	1.4068	1.7899	8.9374	37.9
a, DFT/B3LYP	1.4096	1.3893	1.4361	1.4466	1.4189	1.3849	1.4381	1.7836	9.0227	0.1
e, TD-DFT/B3LYP	1.4117	1.3836	1.4461	1.4303	1.4214	1.3778	1.4512	1.7637	8.9200	0.0
e, TD-DFT/CAM	1.3938	1.3841	1.4081	1.4548	1.4126	1.4026	1.4142	1.7345	8.8093	13.3
e, CCS	1.4023	1.3725	1.4435	1.4118	1.4142	1.3653	1.4491	1.7550	8.8685	0.0
e, ADC(2)	1.4110	1.4075	1.4298	1.4560	1.4280	1.4301	1.4429	1.7485	8.9116	0.0
e, CC2	1.4131	1.4093	1.4317	1.4549	1.4303	1.4308	1.4440	1.7504	8.9193	0.0

Species, Method	C_1C_{11}	$C_{11}C_9$	C_9C_7	C_7C_8	C_2C_{12}	$C_{12}C_{10}$	$C_{10}C_8$	C_2S	C_1S	φ_2
n, CC2	1.4096	1.4076	1.4159	1.4822	1.4124	1.4062	1.4155	1.7861	8.9519	41.3
n, DFT/B3LYP	1.3985	1.3966	1.4075	1.4852	1.4017	1.3952	1.4063	1.7899	8.9374	37.9
a, DFT/B3LYP	1.4096	1.3893	1.4361	1.4466	1.4189	1.3849	1.4381	1.7836	9.0227	0.1
e, TD-DFT/B3LYP	1.4121	1.3835	1.4459	1.4303	1.4211	1.3776	1.4507	1.7637	8.9200	0.0
e, TD-DFT/CAM	1.3890	1.3871	1.4101	1.4548	1.4047	1.4076	1.4244	1.7345	8.8093	12.5
e, CCS	1.4021	1.3727	1.4436	1.4118	1.4128	1.3662	1.4487	1.7550	8.8685	0.0
e, ADC(2)	1.4122	1.4067	1.4292	1.4560	1.4314	1.4279	1.4409	1.7485	8.9116	0.0
e, CC2	1.4139	1.4088	1.4313	1.4549	1.4326	1.4294	1.4429	1.7504	8.9193	0.0

Table S8 Results for 2BMT. The first letters n, a, and e in the left column indicate that the results of the corresponding rows refer to the optimized geometries of the the neutral ground state, anionic ground state, and the lowest excited state of the neutral molecule, respectively. $\varphi_1 \equiv [C_5C_7C_8C_6]$ and $\varphi_2 \equiv [C_9C_7C_8C_{10}]$ represent the torsional angles formed by the two planes specified by the C atoms indicated in the square brackets. Notice that TD-DFT calculations using the functional CAM-B3LYP (labeled TD-DFT/CAM in this table) fail to predict a planar molecular conformation of 2BMT in its lowest excited state. Atom labeling is indicated in Figure 1B. Throughout, lengths are given in angstrom and angles in degrees.

Species, Method	NC_3	C_3C_5	C_5C_7	C_7C_8	C_2C_4	C_4C_6	C_6C_8	C_2S	C_1S	φ_1
n, CC2	1.3568	1.4063	1.4136	1.4802	1.4143	1.4047	1.4152	1.7844	8.9698	39.1
n, DFT/B3LYP	1.3404	1.3960	1.4052	1.4829	1.4032	1.3937	1.4065	1.7882	8.9429	35.8
a, DFT/B3LYP	1.3563	1.3854	1.4356	1.4400	1.4172	1.3850	1.4376	1.7879	9.0374	0.0
e, TD-DFT/B3LYP	1.3534	1.3863	1.4366	1.4392	1.4207	1.3797	1.4456	1.7633	8.9349	0.0
e, CCS	1.3331	1.3761	1.4342	1.4138	1.4191	1.3631	1.4507	1.7470	8.8602	0.0
e, ADC(2)	1.3658	1.3950	1.4492	1.4231	1.4348	1.3866	1.4596	1.7433	8.9450	0.0
e, CC2	1.3578	1.4080	1.4267	1.4576	1.4300	1.4367	1.4467	1.7469	8.9491	0.5

Species, Method	NC_{11}	$C_{11}C_9$	C_9C_7	C_7C_8	C_2C_{12}	$C_{12}C_{10}$	$C_{10}C_8$	C_2S	C_1S	φ_2
n, CC2	1.3568	1.4063	1.4136	1.4802	1.4128	1.4056	1.4145	1.7844	8.9698	39.1
n, DFT/B3LYP	1.3403	1.3960	1.4052	1.4829	1.4022	1.3945	1.4060	1.7882	8.9429	35.8
a, DFT/B3LYP	1.3564	1.3854	1.4356	1.4400	1.4172	1.3850	1.4376	1.7879	9.0374	0.0
e, TD-DFT/B3LYP	1.3534	1.3863	1.4366	1.4393	1.4198	1.3794	1.4462	1.7633	8.9349	0.0
e, CCS	1.3328	1.3763	1.4342	1.4138	1.4176	1.3639	1.4507	1.7470	8.8602	0.0
e, ADC(2)	1.3663	1.3949	1.4490	1.4231	1.4352	1.3845	1.4591	1.7433	8.9450	0.0
e, CC2	1.3616	1.4066	1.4254	1.4576	1.4379	1.4367	1.4413	1.7469	8.9491	0.7

Table S9 Results for BMT-PY. The first letters n, a, and e in the left column indicate that the results of the corresponding rows refer to the optimized geometries of the the neutral ground state, anionic ground state, and the lowest excited state of the neutral molecule, respectively. $\varphi_1 \equiv [C_5C_7C_8C_6]$ and $\varphi_2 \equiv [C_9C_7C_8C_{10}]$ represent the torsional angles formed by the two planes specified by the C atoms indicated in the square brackets. Atom labeling is indicated in Figure 1C. Throughout, lengths are given in angstrom and angles in degrees.

Molecule	ε_{vert}^{CC2}	ε_{ad}^{CC2}	ε_{vert}^{CCS}
44BPY	4.69444	4.10027	5.68435
BMT-PY	4.63776	4.26078	5.26983
2BMT	4.52980	4.25090	5.17698

Table S10 Vertical (subscript *vert*) and adiabatic (subscript *ad*) excitation energies computed by *ab initio* methods indicated by subscripts. Notice that the CCS-based excitation energies are substantially overestimated.